# International Journal of Engineering Research and Science & Technology

ISSN : 2319-5991
Vol. 1, No. 2
April 2015

2nd National Conference on "Recent Advances in Science Engineering & Technologies" RASET 2015

Organized by

Department of EEE, Jay Shriram College of Technology, Tirupur, Tamil Nadu, India.



www.ijerst.com

Email: editorijerst@gmail.com or editor@ijerst.com

International Journal of Engineering Research and Science & Technology

*ISSN 2319-5991 www.ijerst.com*
*Special Issue, Vol. 1, No. 2, April 2015*
*2nd National Conference on "Recent Advances in Science, Engineering&Technologies" RASET-2015*


*Research Paper*

# DIODE FREE T-TYPE THREE-LEVEL NEUTRAL POINT CLAMPED INVERTER FOR LOW VOLTAGE SYSTEMS

**R Gnanasekaran[1]*, K Ganeshkumar[1], P Deepak[1] and R Periyasamy[1]**

**Corresponding Author:* ***R Gnanasekaran***

In this paper, the conventional I- and T-type three-level neutral-point-clamped (3L-NPC) inverter for low-voltage renewable energy systems is investigated. Literature research shows that the T-type inverter improves I-type's insulated-gate bipolar transistor (IGBT) + IGBT current paths. However, the IGBT + diode paths are the same. The calculation in this paper further reveals that the IGBT + diode current paths dominate the conduction losses and even the whole semiconductor losses. Based on the aforementioned recognitions, a novel T-type inverter is presented as an alternative to be applied in the low-voltage renew-able energy systems. In the proposed 3L-NPC, Power Mosfets replace the IGBT + diode middle bidirectional switch. In the proposed topology, there is no diode involved in the current path supposing the unity power factor. In this way, the conduction loss is expected to be reduced compared with that from the conventional T-type 3L-NPC, particularly in the low and medium power range applications.

***Keywords:*** I-types and T-types, Loss, Reduce, Three levels

## INTRODUCTION

Over the past two or three decades, multilevel inverters, such as the neutral-point-clamped (NPC) inverter , the flying capacitor inverter, and the cascaded multilevel converter , have been increasingly studied and widely ap-plied. Multilevel inverters are basically composed by an array of power components and dc voltage supplies which can produce stepped voltage waveforms. Among them, the NPC inverter is the most widely known and adopted multilevel topology for its low current distortion and high efficiency. In the low-voltage renewable energy systems, the three-level NPC (3L-NPC) inverter has been the center of numerous research studies and applications.

In this paper, the state of the art of 3L-NPC inverters applied in the low-voltage renewable energy systems is investigated thoroughly. Moreover, the 3L-NPC inverters are divided into I- and T-types according to their leg shapes. tiveness of those two types for low-voltage renewable energy systems is then discussed.

In the following sections, the leg switch statuses of 1100 and 0011 are defined as nonzero

[1] Department of Electrical & Electronics Engineering,Jay Shriram Group Of Institutions, Tirupur– 638 660.

vectors with positive and negative output voltages, where 0 and 1 denote the switch ON and OFF states, respectively, in the sequence of S1, S2, S1c, and S2c.

The literature shows that the T-type 3L-NPC improves the conduction loss of the nonzero-vector current path of I-type 3L-NPC. However, the zero-vector current path's conduction losses are the same. In both I- and T-type's zero vectors, there are one diode and one insulated-gate bipolar transistor (IGBT) involved in the current path. Therefore, there is at least 2-V total conduction voltage due to IGBT + diode structure according to the IGBT and diode datasheets. Moreover, this conduction voltage causes high power losses, particularly in low and medium power ranges of a renewable energy system.

Moreover, this paper theoretically proves that the zero vec-tor's duty time or its conduction loss is almost equal to the sum of the other positive and negative nonzero vectors. Therefore, the improvement on the zero vector's conduction loss is critical for improving the inverter efficiency.

Based on the aforementioned recognitions, a novel diode-free T-type 3L-NPC inverter for low-voltage renewable energy systems is proposed in this paper, aiming to improve the zero-vector conduction loss and, hence, to reduce the total power loss.

In this new topology, a Power Mosfet paralleled path is formed as the zero-vector current path. There is no diode involved in the zero-vector current paths even with the nonunity power factor. Instead, two reverse conducted Power Mosfets are used as diodes. Therefore, the zero vector's conduction voltage is reduced a lot and ranged from a few hundred millivolts up to about 2 V with the rated power. Since there is no IGBT body diode

**Figure 1: Conventional I-type 3L-NPC**

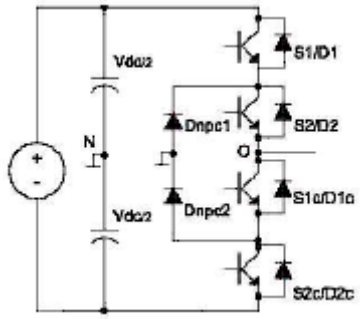


conducted as well supposing the unity power factor, the new topology can be defined as diode-free T-type 3L-NPC.

**Figure 2: Current Paths of Convetional I-type 3L-NPC leg. (a) 1100, (b) 0110, (c) 0011**

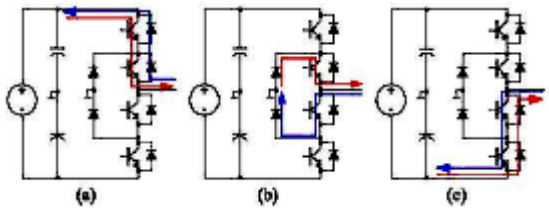


This rest of this paper is organized as follows. In Section II, various kinds of 3L-NPC inverters are analyzed and classified into I- and T-types. The common high zero-vector conduction losses of both are summarized. Based on the discussion in Section II, a novel T-type 3L-NPC topology, together with its pulse width - modulation (PWM) strategy, is proposed and de-scribed in Section III. In Section IV, the power loss distribution is evaluated among the conventional T-type 3L-NPC and the proposed T-type 3L-NPC. Later in Section V, the system design and experimental results are discussed for the case where these new topology is applied to a solar inverter system. Finally, Section VI concludes this paper.

**Figure 3: Long Commutation Path During Reactive Power Generation**

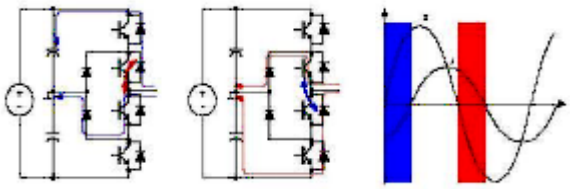

## INVESTIGATION OF 3L-NPC INVERTER FOR RENEWABLE ENERGY SYSTEM

Currently, I-type 3L-NPC has been studied and applied dom-inantly in low-voltage renewable energy systems. We proposed a three-level active clamped NPC inverter used for renewable energy systems to improve the efficiency. The 3L-NPC wind converter's operation strategy under unbalanced grid condition is discussed in. We proposed a split inductor I-type 3L-NPC in the solar system for low leakage current and dead-time elimination. A novel highly efficient stacked 3L- NPC (3L-SNPC) inverter is proposed in to provide the paralleled current paths. Based on the work in We in proposed an active clamped 3L-SNPC to further distribute power losses evenly. The aforementioned literature covers the different perspec-tives of I-type 3L-NPC. However, all hardware topologies are based on or derived from the fundamental I-type 3L-NPC leg.

**Figure 4: One leg of the T-type 3L-NPC**

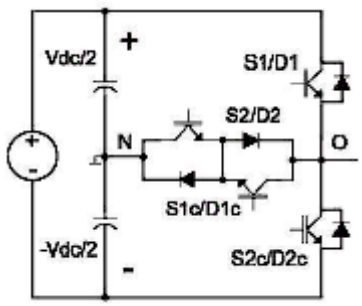


Therefore, they have common or similar features, as de-scribed in the following.

Figure. 2 shows the current paths with the leg switch statuses of 1100, 0110, and 0011. As aforementioned, 1100 and 0011 are defined as nonzero vectors with the output voltage being equal to ±*V*dc/2, and 0110 is defined as a zero vector with output equal to zero.

It is shown in Figure. 2 that, in both zero vector and nonzero vector, the current paths include two power devices. These long current paths imply the high conduction loss. Second, higher stray inductance, due to the long current paths, results in higher power loss and turns off over voltages.

Moreover, Figure. 3 shows the reactive power generation of the conventional I-type 3L-NPC. In the blue and red regions of Figure. 3, when the switching sequence changes from 1100 to 0110, or from 0011 to 0110, the current commutates through a long commutation path from D1, D2 to S1c, Dnpc2 or from D1c, D2c to S2, Dnpc1. Therefore, four devices are involved in the current commutation. The longer commutation paths consisting of four devices cause higher power transition loss as well as the higher conduction loss. Having the same arguments with the aforementioned long current path, the long commutation path in Figure. 3 increases the stray inductance. More importantly, there are three diodes involved when a zero vector is commutating with a nonzero vector. It causes higher diode reverse recovery losses and worse electromagnetic interference issues.

It is worthy of noting that the renewable energy system is usually operating in a much lower power range than the rated power. Moreover, the foregoing discussed drawbacks of I-type 3L-NPC seem more prominent because of the IGBT and

diode relatively larger state voltage/current ratio at the low and medium powers.

Based on the foregoing recognitions, the T-type 3L-NPC, as shown in Figure. 4, is being studied increasingly to improve the system efficiency. We in evaluated the power loss and control scheme of T-type 3L-NPC applied in the low-voltage renewable energy system. We in [11] applied T-type 3L-NPC in a solar system to avoid the high conduc-tion loss.

As shown in Figure. 5, in the T-type 3L-NPC, the long current paths of nonzero vectors [as shown in Figure. 2(a) and (c)] are shortened with only one device conducting. Therefore, the con-duction loss of the T-type 3L-NPC in states shown in Figure. 5(a) and (c) is smaller than that of the I-type.

Moreover, the reactive power current commutation paths, as shown in Figure. 6, reveal that one diode is less involved in the current commutation compared to I-type 3L-NPC.

However, the same as in I-type 3L-NPC, the zero-vector 0110 in Figure. 5(b) has IGBT + diode two power devices conducting in the current paths with up to 4 V of the ON-state voltage. The high ON-state voltage can cause the same high conduction loss as the I-type 3L-NPC shown in Figure. 2(b), particularly in low and medium power ranges. More importantly, it should be emphasized that, in Figures. 2 and 5, the zero vector in (b) occurs about as much as the sum

**Figure 5: Topological States of T-type 3L-NPC. (a) 1100 (b) 0110 (c) 0011**

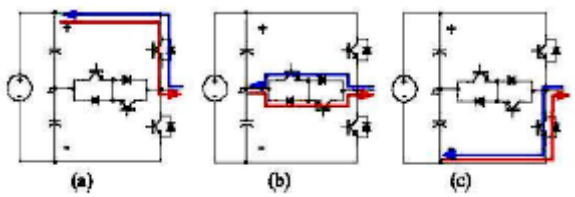


of the nonzero vectors in (a) and

(c), as aforementioned. Therefore, the zero vector dominates the conduction loss more than the nonzero vector. From this point of view, the improvement of T-type 3L-NPC over I-type 3L-NPC is much limited. The verification is given as follows.

As shown in Figure. 7, assume that the number of isosceles triangles in the first 1/4 of the sine modulation wave, namely, $\pi/2$, is $N$. Then,

**Figure 6: Topological States of T-type 3L-NPC within the Reactive Power Region**

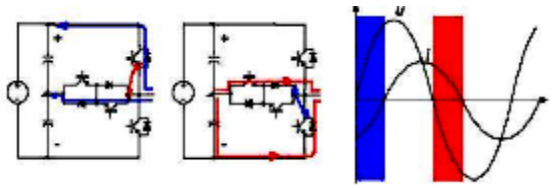

the number of triangular half-waves is $2N$.

In the $k$th triangular half-wave, we have

$$\overline{AB} = m \cdot \sin\left(\frac{k}{2N} \cdot \frac{\pi}{2}\right) \tag{1}$$

where $m$ is the modulation ratio.

$$\overline{BD} = \frac{\overline{AB}}{\overline{AC}} \cdot \overline{CE} = \frac{m \cdot \sin\left(\frac{k}{2N} \cdot \frac{\pi}{2}\right)}{1} \cdot \frac{\frac{\pi}{2}}{2N} \text{ (rad)} \tag{2}$$

where $\overline{CE} = (\pi/2)/2N$ (rad).

Therefore, the sum of the high level in 1/4 cycle is

$$x = \sum_{k=1}^{2N} m \cdot \sin\left(\frac{k}{2N} \cdot \frac{\pi}{2}\right) \cdot \frac{\pi}{4N} \text{ (rad)}. \tag{3}$$

Assuming that $t = k/2N$, then

$$x = \frac{\pi}{4N} \cdot m \cdot \int_0^1 \sin\left(t \cdot \frac{\pi}{2}\right) \cdot 2N dt = m \text{ (rad)}. \tag{4}$$

If $m$ = 0.86, in the first 1/4 of a sine wave,

**Figure 7: kth Triangular Half-wave**

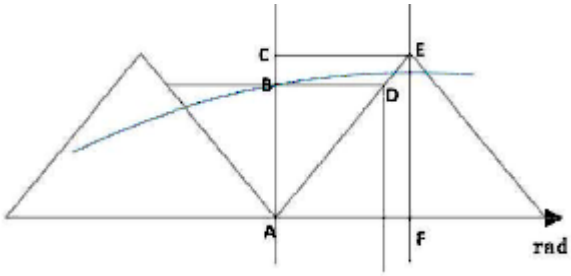


namely, $\pi/2 \sim 1.57$ rad, the sum of the high level is 0.86 rad. Therefore, the zero vector's duty time reaches 45%, which is only 10% less than the total time of the nonzero vectors. The power loss calculation shows that the zero-vector conduction loss could be larger if the power factor is less than unity, which means that, in a sinusoidal cycle, the proportion of state (b) is nearly the same as the sumof state (a) and state (c) in Figures. 2 and 5.

To summarize, in both I- and T-type 3L-NPCs, the zero vector's conduction loss dominates the whole conduction losses and even the whole conventional T-type 3L-NPC only improves the I-type nonzero-vector conduction losses, and the current path of T-type zero vector is the same as that of I-type. Therefore, the T-type improvement over I-type is much limited due to the unimproved zero-vector conduction loss.

**Figure 8: Proposed Novel T-type 3L-NPC**

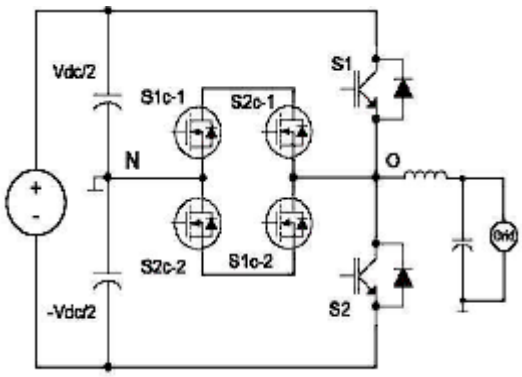


In this paper, based on the aforementioned recognitions of the conventional 3L-NPC, a novel diode-free T-type 3L-NPC inverter is proposed, aiming to reduce the zero-vector conduc-tion loss, particularly in the low and medium power ranges.

## PROPOSED DIODE-FREE T-TYPE 3L-NPC INVERTER AND ITS PWM STRATEGY

The proposed novel diode-free T-type 3L-NPC inverter for low-voltage renewable energy systems is shown in Figure. 8.

In this new topology, two 600-V Power Mosfets in the reverse serial connection, hence S1c-1&S2c-1 and S2c-2&S1c-2, re-place the IGBT + diode bidirectional middle switch in the conventional T-type 3L-NPC. Thus, in this topology, four Power -Mosfets form a parallel current path to reduce the equivalent ON-state resistance. More importantly, the zero-vector current. flows through two Power Mosfets in the reverse connection; hence, no body diode is involved in the current path even with the nonunity power factor.

The PWM strategy for the new topology is shown in Figure. 9.

With the new PWM strategy, the corresponding topological states with the unity power factor. The cur-rent commutation within the reactive power generation region.

The conduction features of the parallel Power Mosfets struc-ture, the power Mosfet + diode, and the conventional IGBT + diode switches in T-type 3L-NPC are tested and plotted in Figure. 12 for comparison. In Figure.11, the IGBT + diode

structure's conduction voltage ranges from 2 to 4 V. However, the new par-allel structure can soundly reduce the zero vector's conduction voltage to less than 2 V, particularly in the low current range. The power Mosfet + diode structure can reduce the ON-state voltage within low and medium power ranges compared with IGBT + diode. However, it causes larger conduction losses in the high power range.

Moreover, in Figure. 10, with the unity power factor, there is no body diode involved when a zero vector is commutating with a nonzero vector. Even in Figure. 11, with the nonunity power factor, there is only one diode involved in the current commutation, while there are three and two diodes involved in the conventional I- and T-type 3L-NPCs, respectively.

**Figure 9: PWM Strategy**

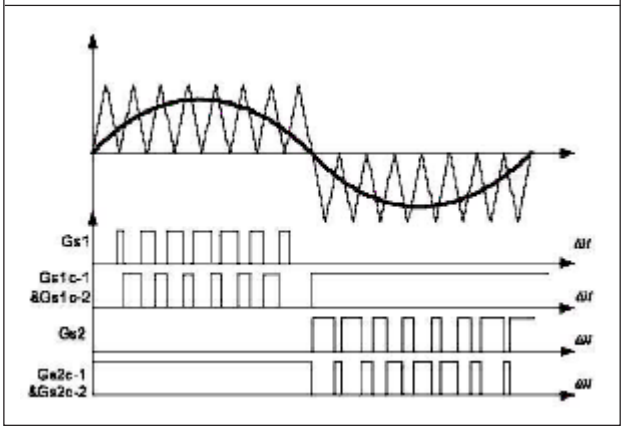


**Figure 10: Topological States with Unity Power Factor (a) $V_a=0$ (b) $V_a=V_{dc}/2$ (c) Va=0 (d) $-V_{dc}/2$**

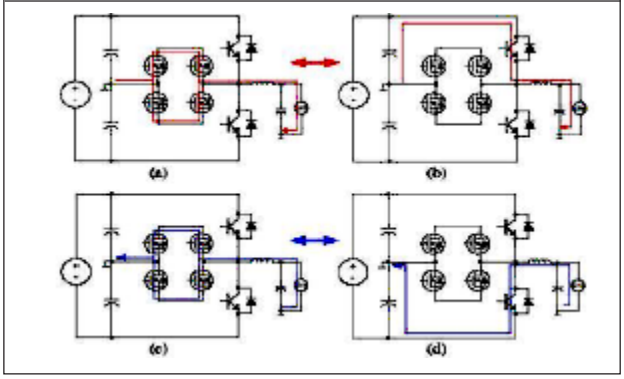


**Figure 11: Current Commutation within the Reactive Power Region**

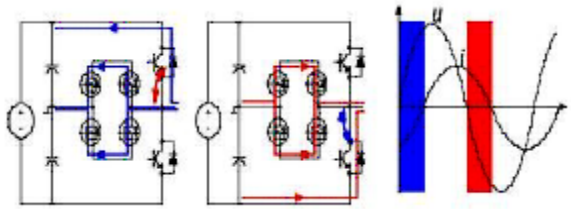

## POWER LOSS EVALUATION

With the nonzero vectors, the con-duction loss is the same as that of the conventional T-type 3L-NPC. However, in the zero vector, the current is flowing through a parallel structure consisting of four Power mosfets, two conducting reversely and two conducting forward. In this way, the equivalent ON-state resistance is half reduced. More importantly, there is no body diode involved in the zero-vector current path.

In order to quantitatively verify the new topology, the semi-conductor losses of the conventional T-type and the novel T-type 3L-NPC under different output power values are calculated.

where ~, *v*FW, *Ug*, $_{Pout,}$ *T*, $_{ron,}$ and *vce* are the phase

$$P_{S1,S2-\mathrm{cond}} = \frac{1}{T}\left(\int_0^{\varphi} v_{\mathrm{FW}}\cdot\left(\frac{P_{\mathrm{out}}\cdot\sqrt{2}\cdot\sin(\omega t)}{U_g}\right)\cdot m\cdot\sin(\omega t)dt + \int_{\varphi}^{\pi} v_{ce}\cdot\left(\frac{P_{\mathrm{out}}\cdot\sqrt{2}\cdot\sin(\omega t)}{U_g}\right)\cdot m\cdot\sin(\omega t)dt\right) \quad (5)$$

$$P_{S1c-1,S1c-2,S2c-1,S2c-2-\mathrm{cond}} = \frac{1}{T}\left(\int_0^{T} r_{\mathrm{on}}\cdot\left(\frac{1}{2}\frac{P_{\mathrm{out}}\cdot\sqrt{2}\cdot\sin(\omega t)}{U_g}\right)^2 \times(1-m\cdot\sin(\omega t))\,dt\right) \quad (6)$$

angle, IGBT body diode forward voltage, grid voltage, output power, grid period, Power Mosfet

**Figure 12: Drive signals of all six switches**

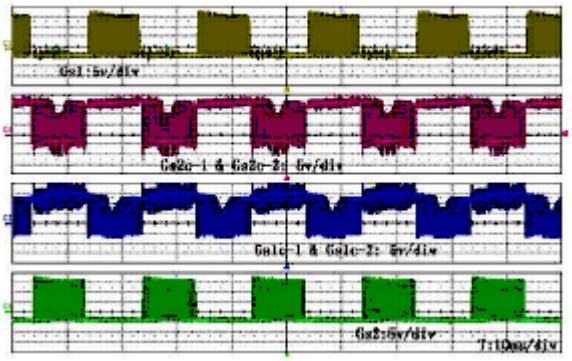

ON-state resistance, and IGBT ON-state voltage, respectively. As (6) shows, the Power Mosfet conduction loss is the same at different power factors or ~.

The switching loss is calculated using the following iterative algorithm *Fs, f,* and *Ts* are the switching frequency, grid frequency, and grid period, respectively, while *E* is the function between the turn-on/turnoff losses per pulse and the current provided in the datasheet.

The power loss calculation results are shown in Figure. 13. It shows that the zero vector's conduction loss is almost equal to the nonzero vector's conduction loss in the conventional T-type 3L-NPC. However, the novel T-type 3L-NPC can soundly reduce the zero-vector conduction loss.

The total conduction loss increases when *m* is reduced. Moreover, the zero-vector con-duction loss proportion increases with the reduced *m. T*he reduced power factor changes the upper and lower IGBT conduction losses due to the body diode. However, the parallel Power Mosfet current path conduction loss does not change with the different power factors.

It is shown that the zero-vector conduction loss is reduced up to 90% by the parallel Power Mosfet current path.

If the switching loss is also counted into the total semicon-ductor loss, it is shown in Figure. 14 that the total semiconductor loss is reduced up to 30% by the improved zero vector. Particularly in the low and medium power ranges with the relatively low efficiency, the efficiency improvement is salient.

## SYSTEM DESIGN AND EXPERIMENTAL RESULTS

A 24V, 6A solar inverter is designed to verify the new T-type 3L-NPC inverter. The current controller and the PWM strategy as shown in are implemented by a low-cost DSP.

The experimental results are shown from with the unity power factor.

Figure. shows the drive signals of all six switches. It shows that, in the zero vector, all four Power mosfets are on to form a bidirectional middle switch. It should be mentioned that, in channels 2 and 3, the drive signals of Gs2c-2 and Gs1c-2 are the same as those of Gs2c-1 and Gs1c-1, and then de-noted by Gs2c-1 and Gs1c-1 due to the channel and probe limitation. Figures. 18 and 19 show the drive signals of Gs1, Gs1c-1, and Gs1c-2 and the grid-side voltage and current at 2.5 and 5 kW, respectively. Figure. shows the efficiency plot in all power range and the comparison with the conventional T-type 3L-NPC solar inverter. It shows that the efficiency, particularly in the low In this paper, a novel diode-free zero-vector loss-reduced power range, is soundly improved.

## REFERENCES


1. Maheshwari R, Munk-Nielsen S, and Busquets-Monge S (2013), "Design of neutral-point voltage controller of a three-level NPC inverter with small DC-link capacitors," *IEEE Trans. Ind. Electron.,* Vol. 60, No. 5, pp. 1861– 1871.
2. Petrella R, Buonocunto N, Revelant A, and Stocco P (2011), "DC bus volt-age equalization in single-phase split-capacitor three-level neutral-point-clamped half-bridge inverters for PV applications," in *Proc. IEEE 26th Annu. APEC,* Fort Worth, TX, USA, Mar. 6–11, pp. 931-938.
3. McGrath B P, Holmes D G, and Kong W Y (2014), "A decentralized controller architecture for a cascaded H-bridge multilevel converter," *IEEE Trans. Ind. Electron.,* Vol. 61, No. 3, pp. 1169–1178.
4. Buticchi G, Lorenzani E, and Franceschini G (2013), "A five-level single phase grid-connected converter for renewable distributed systems," *IEEE Trans. Ind. Electron.,* Vol. 60, No. 3, pp. 906–918.
5. Ebrahimi J, Babaei E, and Gharehpetian G B (2012), "A new multi-level con-verter topology with reduced number of power electronic components," *IEEE Trans. Ind. Electron.,* Vol. 59, No. 2, pp. 655–667.
6. Veenstra M and Rufer A (2005), "Control of a hybrid asymmetric multilevel inverter for competitive medium-voltage industrial drives," *IEEE Trans. Ind. Appl.,* Vol. 41, No. 2, pp. 655–664.
7. Soeiro T B and Kolar J W (2013), "The new high-efficiency hybrid neutral-point-clamped converter," *IEEE Trans. Ind. Electron.,* Vol. 60, No. 5, pp. 1919–1935.
8. Cavalcanti M C, Farias A M, Oliveira K C, Neves F A S, and Afonso J L (2012), "Eliminating leakage currents in neutral point clamped inverters for photovoltaic systems," *IEEE Trans. Ind. Electron.,* Vol. 59, No. 1, pp. 435–443.
9. Wang Y and Li R (2013), "Novel high-efficiency three-level stacked neutral point clamped grid tied inverter," *IEEE Trans. Ind. Electron.,* Vol. 60, No. 9, pp. 3766–3774.
10. Schweizer M and Kolar J W (xxxx), "Design and implementation of a highly efficient three-level T-type converter for low-voltage applications," *IEEE Trans. Power Electron.,* Vol. 28, No. 2, pp. 899–907.


International Journal of Engineering Research and Science & Technology
Hyderabad, INDIA. Ph: +91-09441351700, 09059645577
E-mail: editorijlerst@gmail.com or editor@ijerst.com
Website: www.ijerst.com